Supporting Inforamtion

Nickel-molybdenum carbide-based composite catalyst enables CO_2 electroreduction to syngas with accurately adjustable CO/H_2 ratio

Chaofan Zhang,[a] Boyuan Miao [b] and Zhongkui Zhao*[a]

[a]State Key Laboratory of Fine Chemicals, Department of Catalysis Chemistry and Engineering, School of Chemical Engineering, Dalian University of Technology, Dalian 116024, China

[b] PetroChina Dalian Petrochemical Company, Dalian 116000, China

* Corresponding authors. E-mail: zkzhao@dlut.edu.cn.

Supplementary Figures

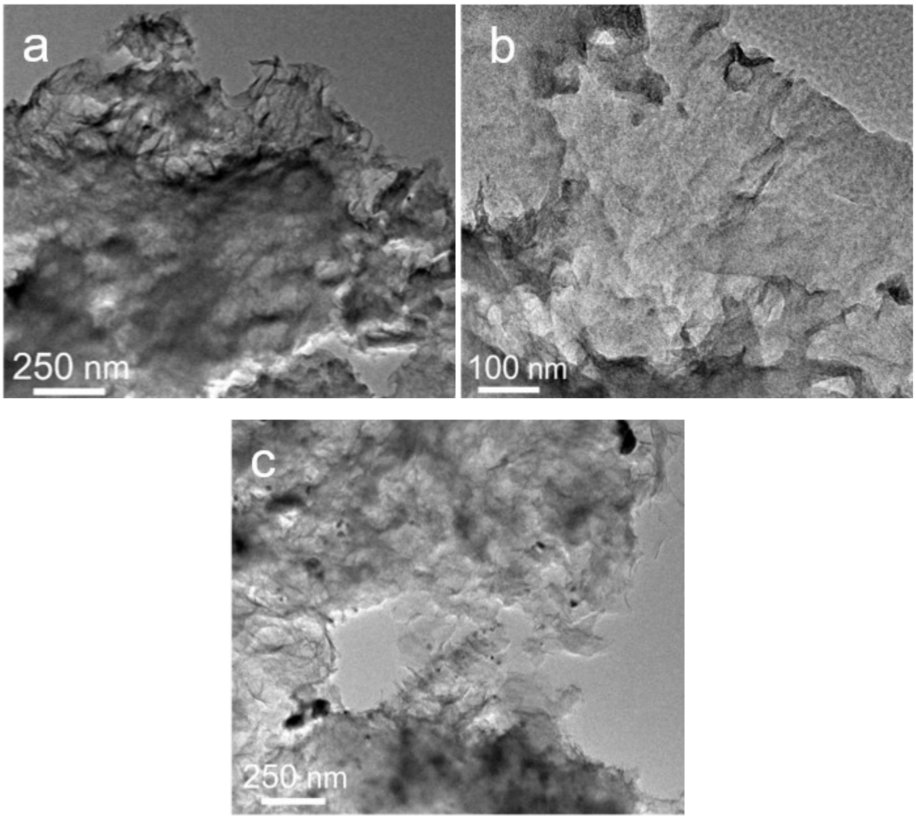

Fig. S1. a-c) The TEM images of Ni/NC (a), MoC/NC (b) and Ni-MoC/NC (c).

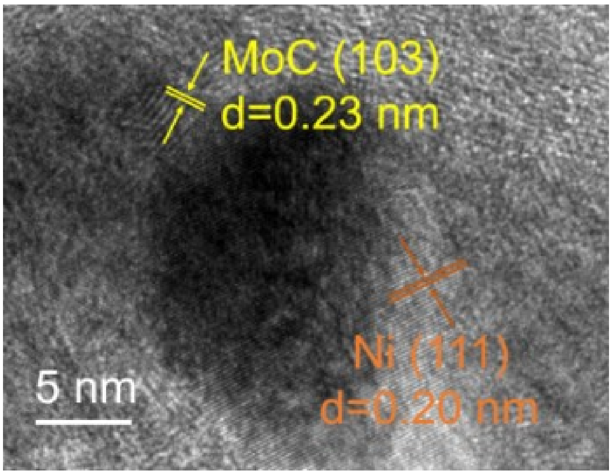

Fig. S2. The HRTEM image of Ni-MoC/NC.

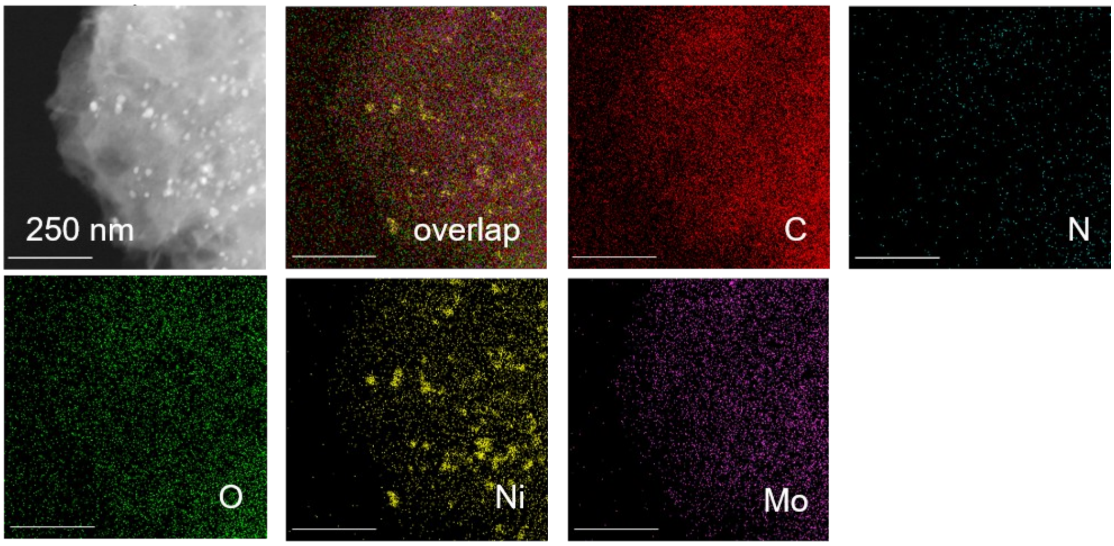

Fig. S3. The EDS mapping of Ni-MoC/NC.

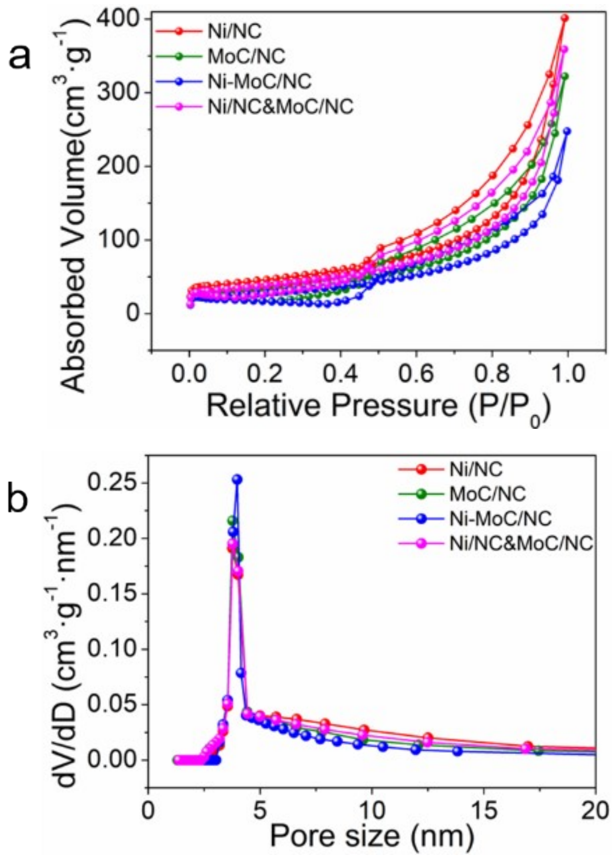

Fig. S4. (a) N_2 sorption isotherms of Ni/NC, MoC/NC, Ni-MoC/NC and Ni/NC&MoC/NC. (b) The pore size distributions of Ni/NC, MoC/NC, Ni-MoC/NC and Ni/NC&MoC/NC.

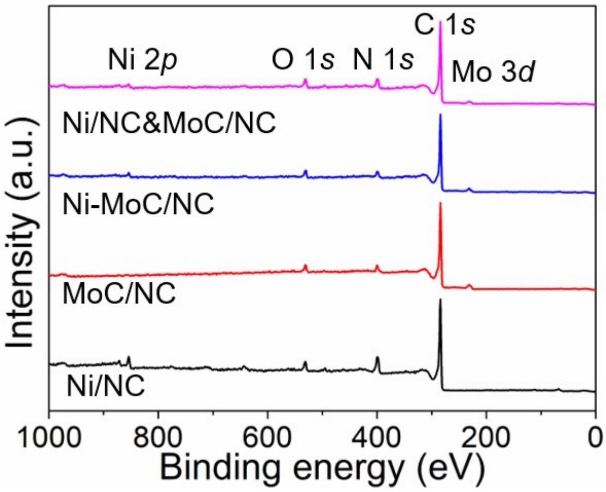

Fig. S5. The XPS survey spectra of Ni/NC, MoC/NC, Ni-MoC/NC and Ni/NC&MoC/NC.

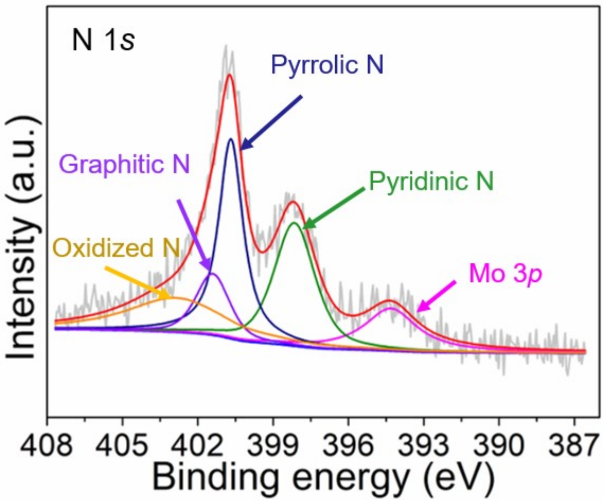

Fig.S6. N 1*s* xps spectra of MoC/NC.

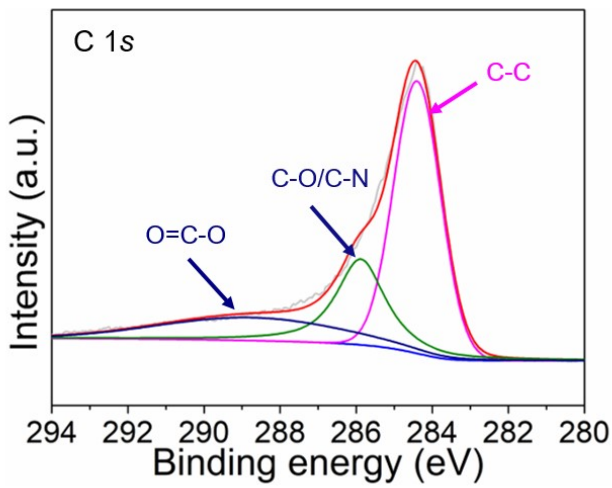

Fig.S7. C 1*s* xps spectra of Ni/NC.

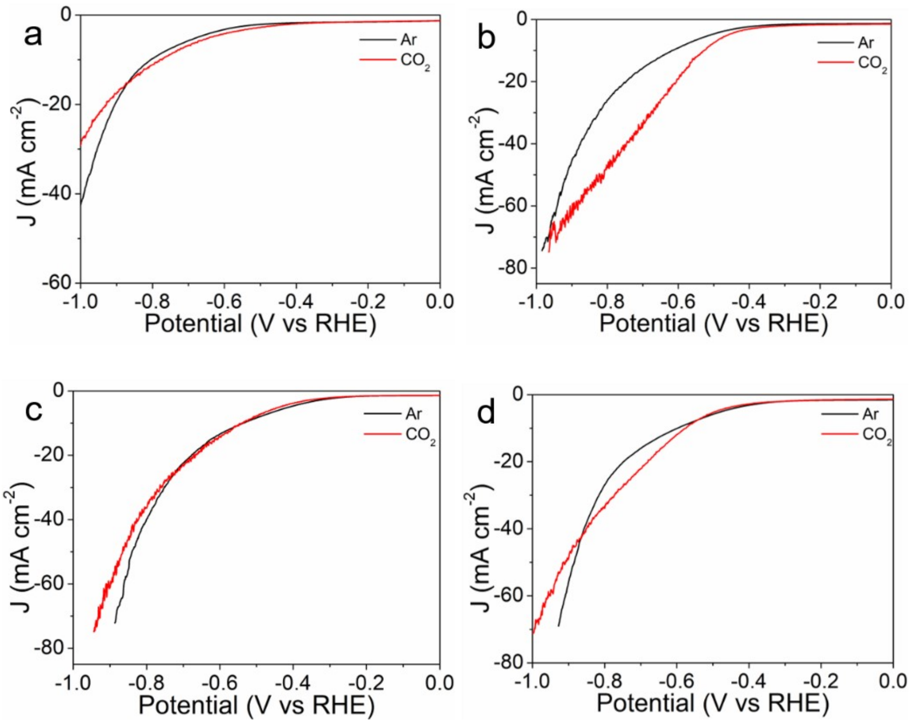

Fig.S8. a-d) LSV curves in Ar or CO_2-saturated 0.5 M $KHCO_3$ solution with a scan rate of 5 mV·s^{-1} of NC (a), Ni/NC (b), MoC/NC (c) and Ni-MoC/NC (d).

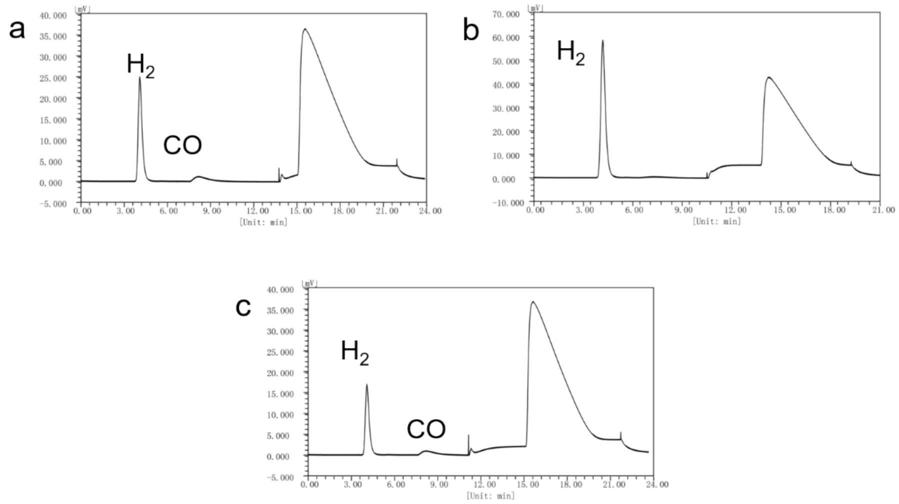

Fig.S9. a-c) Gas chromatograms of CO_2RR products over Ni/NC (a), MoC/NC (b) and Ni-MoC/NC (c) .

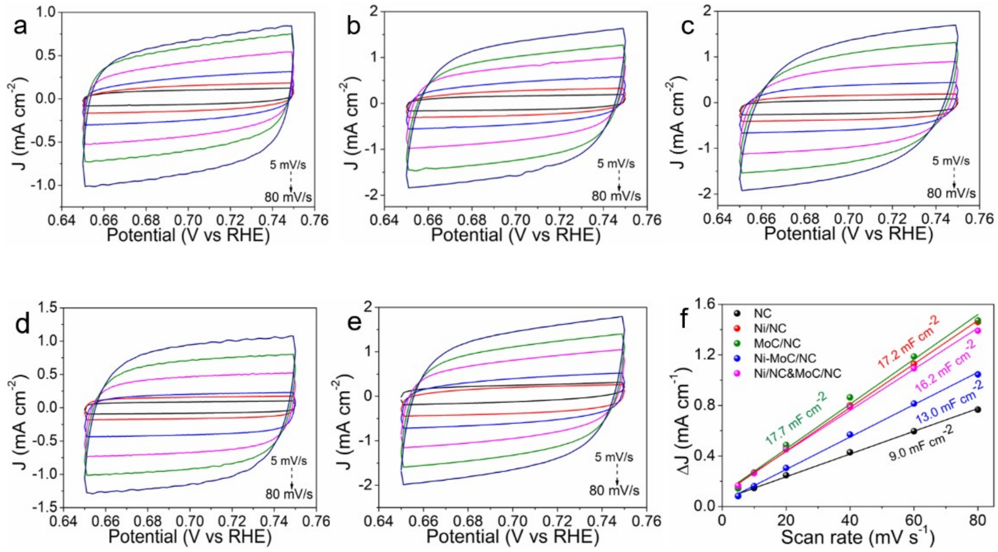

Fig.S10. a-f) CV curves of NC (a), Ni/NC (b), MoC/NC (c), Ni-MoC/NC (d) and Ni/NC&MoC/NC (e) under different scan rates from 5 $mV\cdot s^{-1}$ to 80 $mV\cdot s^{-1}$. (f) Half of the capacitive current density difference as a function of scan rates for NC, Ni/NC, MoC/NC, Ni-MoC/NC and Ni/NC&MoC/NC.

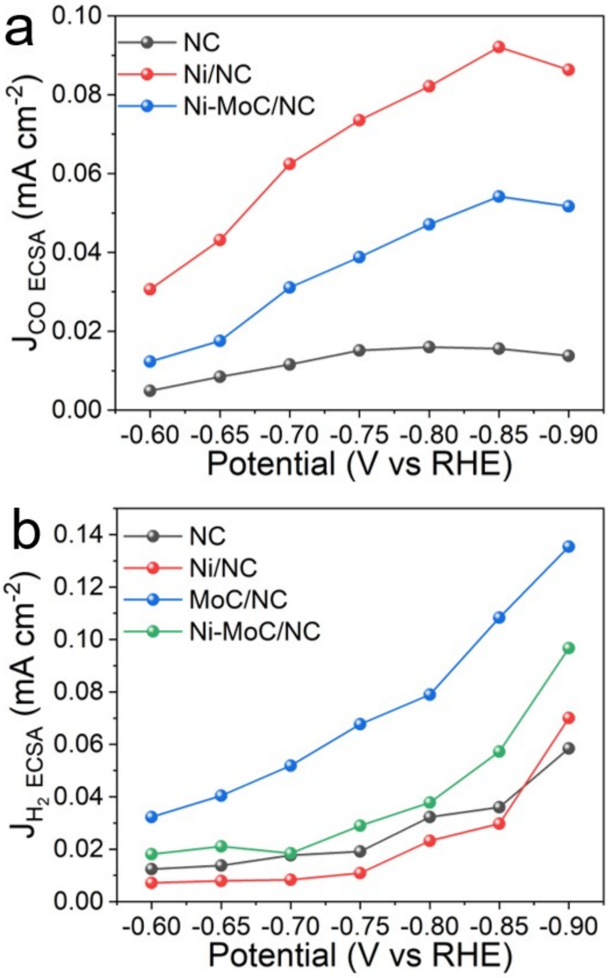

Fig. S11. (a) J_{CO} normalized by ECSA of NC, Ni/NC, and Ni-MoC/NC. (b) J_{H2} normalized by ECSA of NC, Ni/NC, MoC/NC and Ni-MoC/NC.

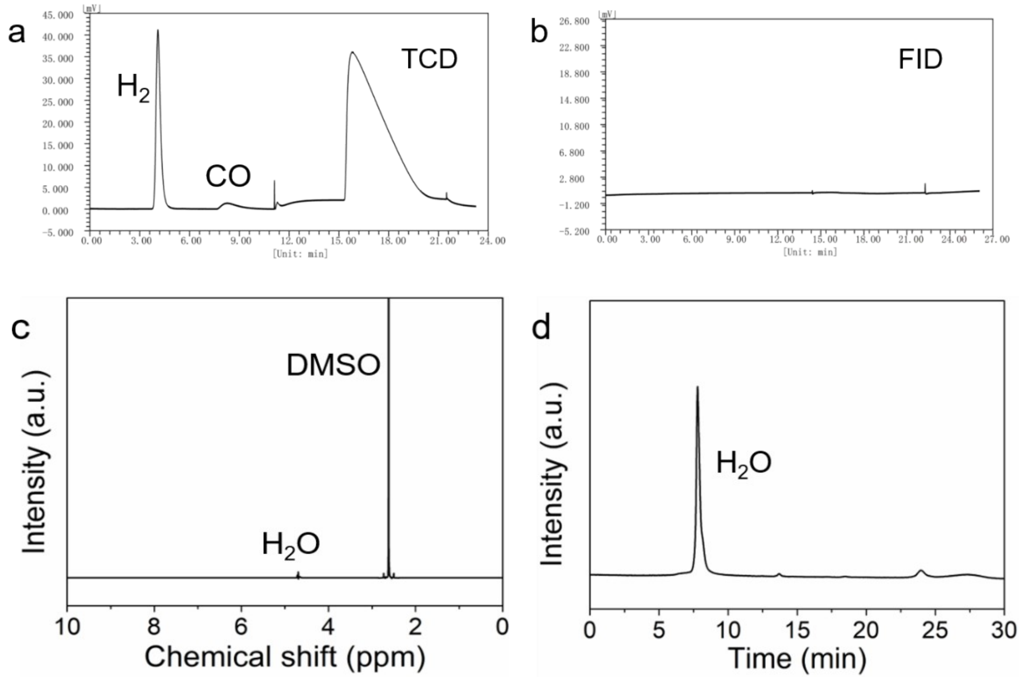

Fig.S12 a,b) Gas chromatograms of the products from the electrocatalytic CO_2RR over Ni/NC&MoC/NC, TCD chromatogram (a), FID chromatogram (b), (c) ^{1}H NMR spectrum, (d) Liquid chromatograms.

Note: Two peaks appear in the liquid chromatogram. One is the water peak at 7.7 min, which has been marked in the figure. The other peak at 23.9 min is an impurity originating from the column.

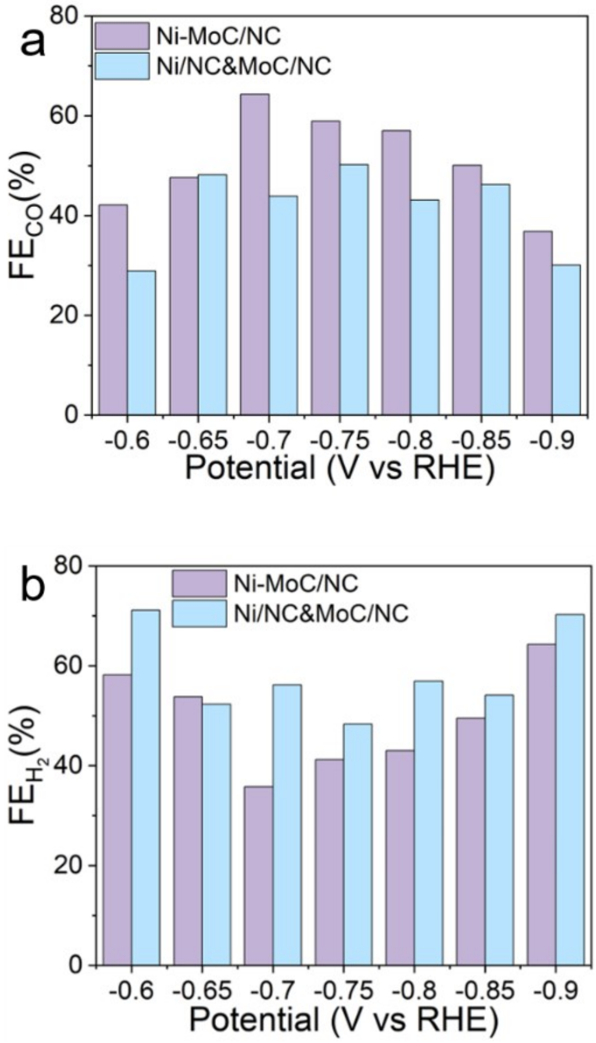

Fig.S13. (a) FE_{CO} of Ni-MoC/NC and Ni/NC&MoC/NC. (b) FE_{H2} of Ni-MoC/NC and Ni/NC&MoC/NC

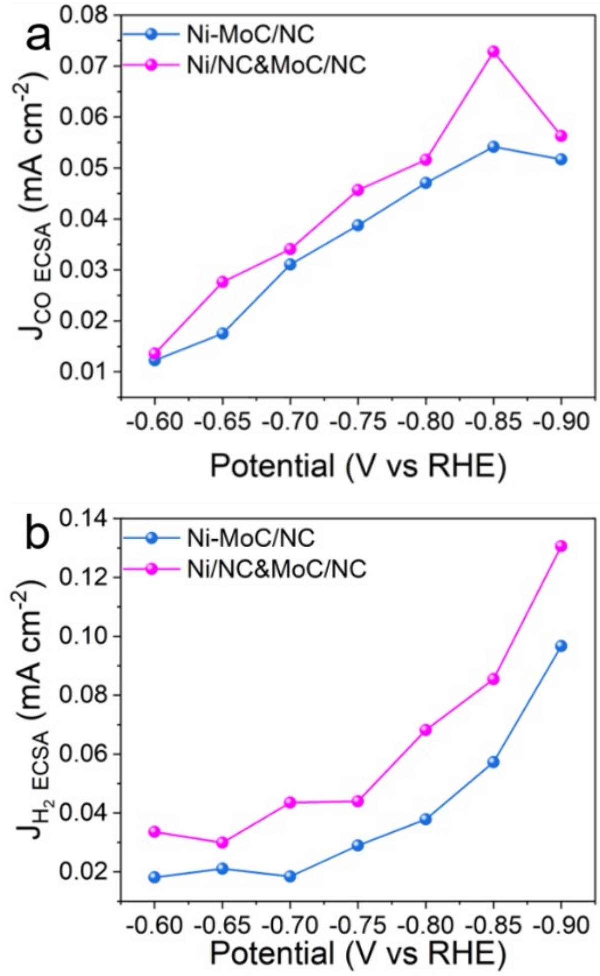

Fig. S14. (a) J_{CO} normalized by ECSA of Ni-MoC/NC and Ni/NC&MoC/NC. (b) J_{H2} normalized by ECSA of Ni-MoC/NC and Ni/NC&MoC/NC.

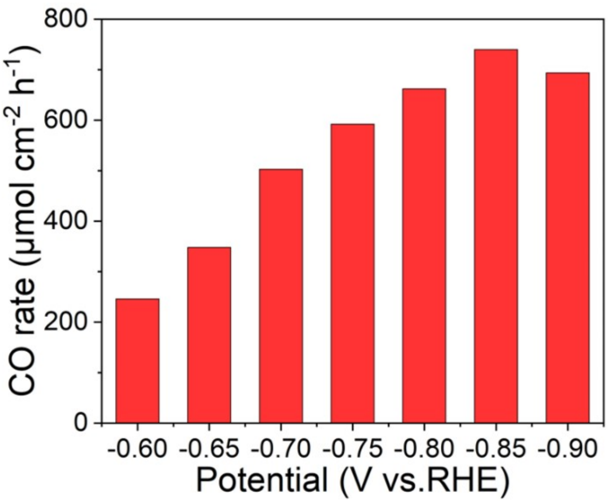

Fig.S15. CO rate of Ni/NC at different potentials

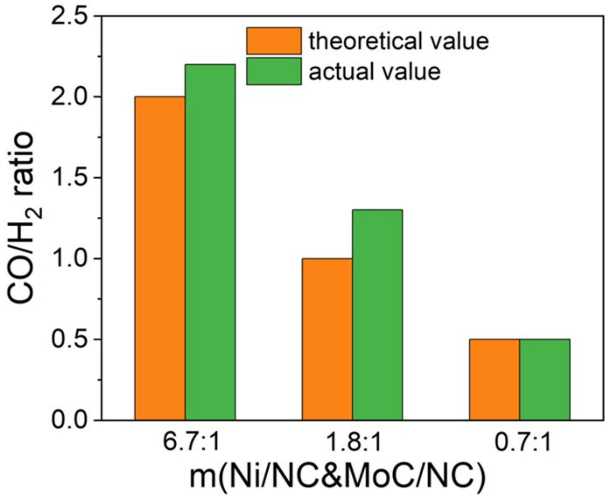

Fig.S16. Theoretical CO/H_2 ratio and actual CO/H_2 ratio corresponding to Ni/NC and MoC/NC theoretical mass ratios at -0.85V vs RHE.

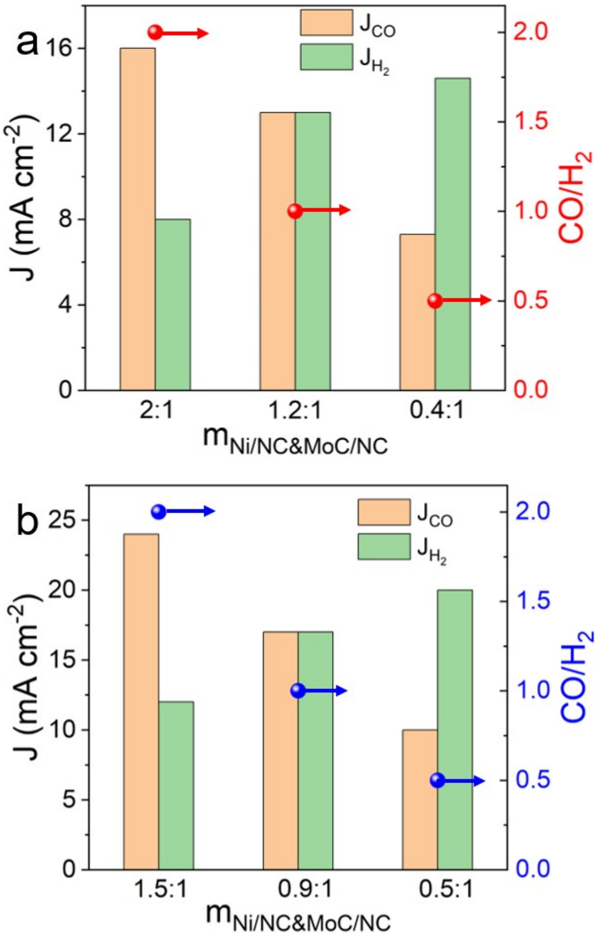

Fig. S17 (a) J_{CO}, J_{H2}, and CO/H_2 ratios for electroduction of CO_2 for syngas production over Ni/NC&MoC/NC catalysts with diverse mass ratio of Ni/NC to MoC/NC including 2:1, 1.2:1 and 0.4:1 under -0.65V vs. RHE, (b). J_{CO}, J_{H2}, and CO/H_2 ratios for electroduction of CO_2 for syngas production over Ni/NC&MoC/NC catalysts with diverse mass ratio of Ni/NC to MoC/NC including 1.5:1, 0.9:1 and 0.5:1 under -0.75V vs. RHE

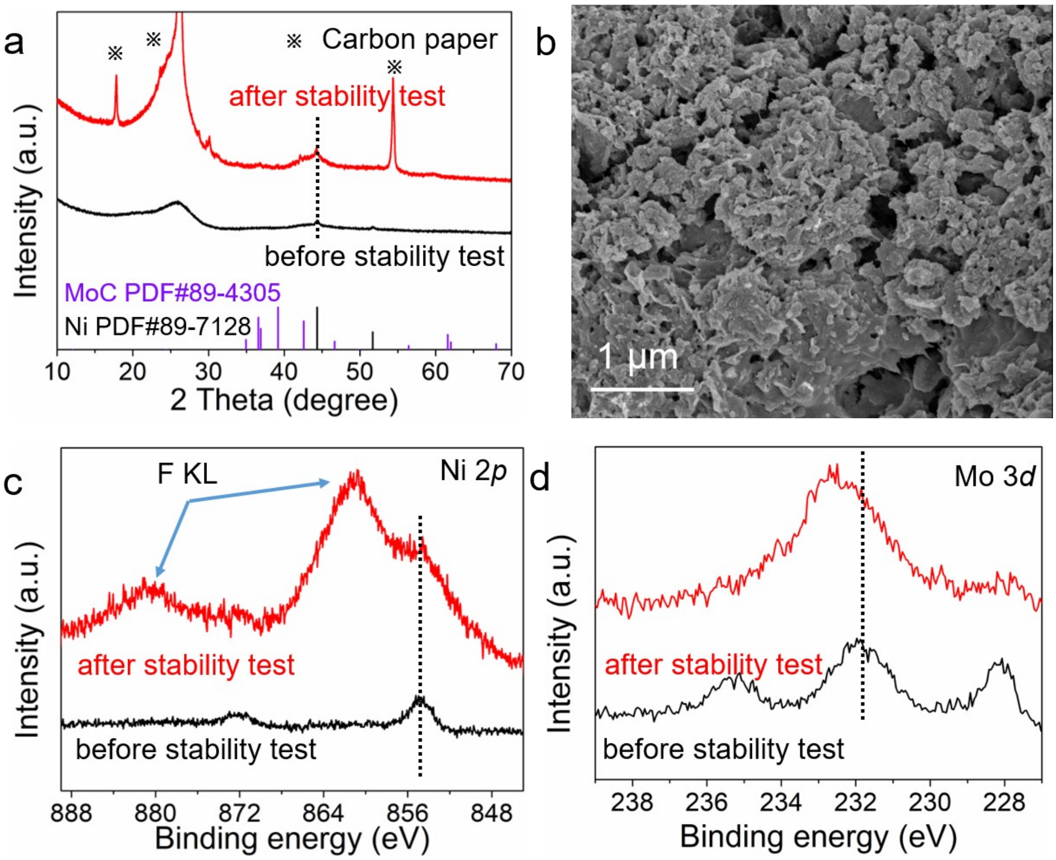

Fig.S18 Characterization of the Ni/NC and MoC/NC catalysts (mass ratio = 1.3:1) after stability testing at -0.85 V vs. RHE (a) XRD, (b) SEM, (c) Ni 2p XPS spectrum, (d) Mo 3d XPS spectrum.

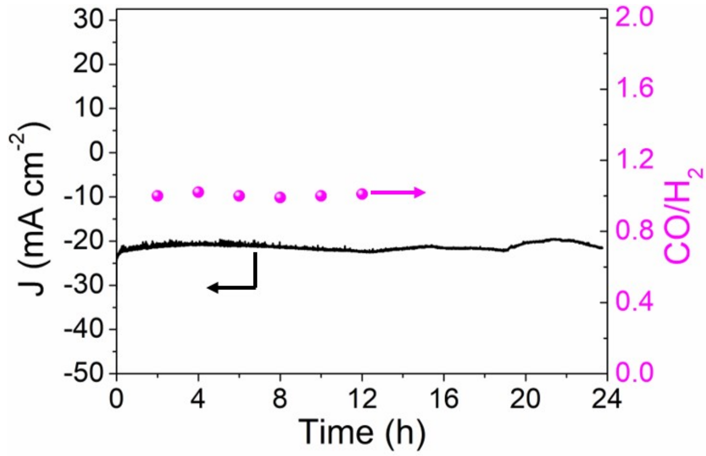

Fig. S19 The chronoamperometry measurement with CO/H_2 ratio over the Ni/NC&MoC/NC composite catalyst with 1.2:1 of mass ratio of Ni/NC to MoC/NC under 0.65V vs RHE. The electrolyte is CO_2-saturated 0.5 M $KHCO_3$ solution.

Supplementary Tables

Table S1. The element content (at%) of the samples was determined by XPS.

Sample	C	N	O	Ni[a]	Mo[b]
Ni/NC	81.16	12.96	4.57	1.31(5.6)	-
MoC/NC	90.29	5.11	3.93	-	0.67(8.3)
Ni-MoC/NC	88.19	5.63	4.75	0.82(3.6)	0.61(5.0)
Ni/NC&MoC/NC	85.97	8.5	4.31	0.83(3.6)	0.39(3.2)

a. The value in parentheses is the calculated Ni weight loadings (wt%) based on the XPS. b.The value in parentheses is the calculated MoC weight loadings (wt%) based on the XPS.

Table S2. CO_2RR to syngas performances of recently reported catalysts in the H-type cell.

Catalysts	E (V vsRHE)	Current density ($mA \cdot cm^{-2}$)	CO/H_2 ratio	Electrolyte	Ref.
$Co_{0.5}Ni_{0.5}$-NC	-0.7	22	1:1	0.5 M $KHCO_3$	1
CoNi-NC	-0.9	51	1:1	0.5 M $KHCO_3$	2
Fe/FeN_4C	-0.45	~5	1:1	0.5 M $KHCO_3$	3
Ni,Fe-hG	-0.9	~15	1:1	0.1 M $KHCO_3$	4
Ni-Fe DASs	-1.1	~75	~1:1	0.5 M $KHCO_3$	5
Cl-Ni/NC	-0.56	6.1	~1:1	0.5 M $KHCO_3$	6
NiNC/FeNC	-0.8	~25	1:1	0.1M $KHCO_3$	7
Co@CoNC-900	-0.8	7.9	1:1	0.1M $KHCO_3$	8
PcCu-O_8-Zn	-1.0	16	1:1	0.5 M $KHCO_3$	9
Cu-Au needle	-0.65	22	1:1	0.5 M $KHCO_3$	10
Ni/NC&MoC/NC	-0.85	52	1:1	0.5 M $KHCO_3$	This work

Table S3. Performance of Ni/NC&MoC/NC with a mass ratio of 1:3 in a flow cell at an applied potential of -0.85 V vs RHE.

J_{CO} (mA·cm^{-2})	J_{H2} (mA·cm^{-2})	CO/H_2
51.2	51.2	1

Reference

1. Y. Chen, M. Xia, C. Zhou, Y. Zhang, C. Zhou, F. Xu, B. Feng, X. Wang, L. Yang, Z. Hu and Q. Wu, *ACS Nano*, 2023, **17**, 22095-22105.
2. Q. He, D. Liu, J. H. Lee, Y. Liu, Z. Xie, S. Hwang, S. Kattel, L. Song and J. G. Chen, *Angew. Chem. Int. Ed.*, 2020, **59**, 3033-3037.
3. Y. Hua, B. Zhang, W. Hao and Z. Gao, *Cell Rep. Phys. Sci.*, 2022, **3**, 100703.
4. J. Leverett, R. Daiyan, L. Gong, K. Iputera, Z. Tong, J. Qu, Z. Ma, Q. Zhang, S. Cheong, J. Cairney, R.-S. Liu, X. Lu, Z. Xia, L. Dai and R. Amal, *ACS Nano*, 2021, **15**, 12006-12018.
5. L. Wang, X. Gao, S. Wang, C. Chen, J. Song, X. Ma, T. Yao, H. Zhou and Y. Wu, *J. Am. Chem. Soc.*, 2023, **145**, 13462-13468.
6. J. Wang, Y. Sun, M. Li, Y. Yi, Q. Liu, Z. Li and L. Wang, *Nano Lett.*, 2025, **25**, 8168-8175.
7. X. Yang, T. Tat, A. Libanori, J. Cheng, X. Xuan, N. Liu, X. Yang, J. Zhou, A. Nashalian and J. Chen, *Mater. Today,* 2021, **45**, 54-61.
8. R. Daiyan, R. Chen, P. Kumar, N. Bedford, J. Qu, J. Cainey, X. Lu and R. Amal, *ACS Appl. Mater. Interfaces*, 2020, **12**, 9307−9315.
9. X. Zhong, M. Ghorbani-Asl, K. Ly, J. Zhang, J. Ge, M. Wang, Z. Liao, D. Makarov, E. Zschech, E. Brunner, I. Weidinger, J. Zhang, A. Krasheninnikov, S. Kaskel, R. Dong and X. Feng, *Nat. Commun.*, 2020, **11**, 1409.
10. M. Ross, C. Dinh, Y. Li, D. Kim, P. Luna, E. Sargent and P. Yang, *J. Am. Chem. Soc.*, 2017, **139**, 9359-9363